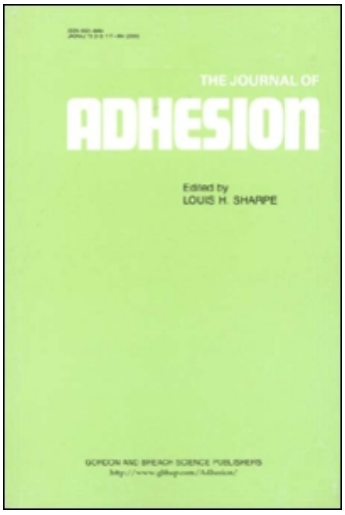

The Journal of Adhesion
Publication details, including instructions for authors and subscription information:
http://www.informaworld.com/smpp/title~content=t713453635

Investigation of Adsorption and Cross-Linking of a Mussel Adhesive Protein Using Attenuated Total Internal Reflection Fourier Transform Infrared Spectroscopy (ATR-FTIR)

Camilla Fant[a]; Julia Hedlund[a]; Fredrik Höök[b]; Mattias Berglin[a]; Erik Fridell[b]; Hans Elwing[a]
[a] Department of Cell and Molecular Biology, Interface Biophysics, Göteborg University, Göteborg, Sweden [b] Department of Applied Physics, Chalmers University of Technology, Göteborg, Sweden

Online publication date: 05 February 2010

To cite this Article Fant, Camilla , Hedlund, Julia , Höök, Fredrik , Berglin, Mattias , Fridell, Erik and Elwing, Hans(2010) 'Investigation of Adsorption and Cross-Linking of a Mussel Adhesive Protein Using Attenuated Total Internal Reflection Fourier Transform Infrared Spectroscopy (ATR-FTIR)', The Journal of Adhesion, 86: 1, 25 — 38
To link to this Article: DOI: 10.1080/00218460903417768
URL: http://dx.doi.org/10.1080/00218460903417768

The Journal of Adhesion, 86:25–38, 2010

ISSN: 0021-8464 print/1545-5823 online
DOI: 10.1080/00218460903417768

Taylor & Francis
Taylor & Francis Group

Investigation of Adsorption and Cross-Linking of a Mussel Adhesive Protein Using Attenuated Total Internal Reflection Fourier Transform Infrared Spectroscopy (ATR-FTIR)

Camilla Fant[1], Julia Hedlund[1], Fredrik Höök[2], Mattias Berglin[1], Erik Fridell[2], and Hans Elwing[1]
[1]Department of Cell and Molecular Biology, Interface Biophysics, Göteborg University, Göteborg, Sweden
[2]Department of Applied Physics, Chalmers University of Technology, Göteborg, Sweden

Mytilus edulis *foot protein 1 (*Mefp-1*) contains the redox-functional amino acid 3,4-dihydroxyphenylalanine (DOPA), which is a typical feature of most mefp proteins. We have previously shown, using combined optic (ellipsometry) and acoustic (QCM-D) measurements, that the oxidizing agent sodium periodate ($NaIO_4$) and the transition metal ion Cu^{2+} promote cross-linking of* Mefp-1*. However, different chemical reaction mechanisms can not be distinguished using these methods. In the present study, we have complemented our previous investigations using Attenuated Total Internal Reflection Fourier Transform Infrared spectroscopy (ATR-FTIR), allowing a spectroscopic analysis of $NaIO_4$ and Cu^{2+}-induced cross-linking of* Mefp-1 *adsorbed on a ZnSe surface. In aqueous solution, adsorbed* Mefp-1 *displays absorption bands at 1570, 1472, 1260, and 973 cm^{-1}. Upon addition of $NaIO_4$ and Cu^{2+}, the absorptions at 1570, 1472, and 973 cm^{-1} increase by approximately a factor of two. In contrast, the band at 1260 cm^{-1} disappears upon cross-linking using $NaIO_4$, but remains unchanged upon addition of Cu^{2+}. This demonstrates that the band at 1260 cm^{-1} is attributed to the C–O stretching vibration of the side chain hydroxyl groups in DOPA and that Cu^{2+} forms complexes with DOPA rather than transform it into an* o*-quinone. Moreover, upon addition of $NaIO_4$ after cross-linking using Cu^{2+}, the band at 1260 cm^{-1} disappears, indicating that the complex formation between DOPA and Cu^{2+} is reversed when DOPA is transformed into the* o*-quinone. These results demonstrate that $NaIO_4$, which initiates a similar reaction to the naturally occurring enzyme catechol oxidase, contributes to the formation of di-DOPA cross-links. In contrast, the dominating contribution to the cross-linking from Cu^{2+}, which is accumulated at high concentrations in the byssus thread of the blue mussel, is* via *complex formation between the metal and DOPA residues.*

Keywords: Adsorption; ATR-FTIR; Cross-linking; *Mefp-1*; Metal binding; Mussel adhesive protein

Received 2 December 2008; in final form 4 August 2009.

One of a Collection of papers honoring J. Herbert Waite, the recipient in February 2009 of *The Adhesion Society Award for Excellence in Adhesion Science, Sponsored by 3 M*.

Address correspondence to Hans Elwing, Department of Cell and Molecular Biology, Interface Biophysics, Göteborg University, Box 462, SE-405 30, Göteborg, Sweden. E-mail: hans.elwing@cmb.gu.se

INTRODUCTION

The common blue mussel attaches itself to underwater solid surfaces using an extracorporal organ known as the byssus. The byssus is a protein-rich (90–95% proteins) [1] bundle of threads connected to the solid surface by adhesive plaques and to the animal through the ventral base of the foot [2]. A detailed understanding about the molecular interactions within and between the involved proteins and their interaction with various solid surfaces is necessary in order to develop strategies that minimize marine fouling [3–10]. It has also been proposed to utilize the adhesive and cohesive properties of the byssal proteins to design biomimetic-inspired biocompatible glues for various medical and dental applications [11,12] and as cell- and tissue-attachment factors [13,14].

The adhesive plaque is composed of at least six different polyphenolic proteins, *Mytilus edulis* foot proteins 1 to 6 (*Mefp-1* to *Mefp-6*) [15–17]. In common for all plaque proteins is that they contain post- or co-translationally hydroxylated and phosphorylated amino acids [16,18–20]. One of the most important hydroxylated amino acids in the plaque proteins is the redox-functional amino acid, 3,4-dihydroxyphenylalanine (DOPA). Apart from being important for the adhesion [21], DOPA also takes part in the cross-linking reaction. The cross-linking involves oxidation of DOPA to a reactive *o*-quinone and, in turn, allows formation of di-DOPA cross-links [22]. The enzyme, catechol oxidase, which has been reported to occur in high levels in mussel byssus, catalyzes this reaction [23]. Another function attributed to DOPA, which may also contribute to the cohesive properties of the byssus, is the ability to form strong complexes (log stability constants >20) with transition metal ions [24,25]. The number of DOPA (one to three) in each complex depends on pH. Metal ions such as Fe, Cu, and Zn are naturally accumulated in the byssal threads of mussels [26,27]. The physiological role of metal accumulation is yet not fully known, but a possible explanation is that the metal incorporation is a consequence of the high level of the amino acid DOPA in the byssus [28]. Another alternative is that the byssal threads function as a disposal system for toxic metals [29]. Recently, it was shown that metal incorporation increased the stiffness of the *Mefp-1* protein [30]. Complex formation between metal ions and two or more DOPA may, thus, in a way similar to the oxidative DOPA-mediated cross-linking, contribute to increased cohesive forces in the byssus by establishing strong protein-protein connections [31,32]. The most extensively studied polyphenolic protein, *Mefp-1*, has been investigated with respect to its molecular structure, physical properties, and adsorption

to surfaces. Although *Mefp-1* undoubtedly contributes to the durability of byssus, it is not directly involved in adhesion. Rather, it provides a robust coating that is four to five times stiffer and harder than the byssal collagens that it covers [30]. Protective coatings for compliant tissues and materials are highly appealing to technology, notwithstanding the conventional wisdom that coating extensibility can be increased only at the expense of hardness and stiffness. Thus, the role of *Mefp-1* in accommodating both parameters deserves further study. Moreover, the *Mefp-1* contains a substantial amount of DOPA and is a good experimental molecule for investigation aspects of adhesion and DOPA-chemistry. *Mefp-1* has a molecular weight of ~110 kD and is composed of 75–85 repeats of decameric and hexameric units. The most frequent decameric unit has the sequence NH_2-Ala-Lys-Pro-Ser-Tyr-Hyp-Hyp-Thr-DOPA-Lys-COOH [33,34]. *Mefp-1* is highly basic and adopts an extended and flexible structure in solution [35,36].

We have previously investigated the adsorption behavior and cross-linking of *Mefp-1* a using quartz crystal microbalance with dissipation monitoring (QCM-D), ellipsometry, and surface plasmon resonance (SPR) [37,38]. As model surfaces, a non-polar CH_3-terminated thiolated gold surface and a negatively charged polar SiO_2 surface were used. The results showed that *Mefp-1* forms a water-rich, flexible, and extended layer when adsorbed on a non-polar surface, whereas it forms a rigidly attached, compact layer on the polar SiO_2 surface. In these studies, cross-linking of the adsorbed proteins was induced by mushroom tyrosinase, sodium periodate ($NaIO_4$), and Cu^{2+}. Mushroom tyrosinase is functionally analogous to mussel catechol oxidase [39] and $NaIO_4$ initiates the same reaction as the enzyme [40]. Cu^{2+} has the ability to form strong complexes with DOPA but can, under certain conditions, also initiate the oxidation of DOPA to the reactive *o*-quinone [41], *i.e.*, the same cross-linking reaction as induced by catechol oxidase and $NaIO_4$. Upon addition of these "cross-linking" agents, the rigidity (shear viscosity and shear elastic modulus) of the adsorbed mussel-protein films increases significantly, accompanied by a significant contraction and release of coupled water [38]. We also studied the formation of molecular aggregates of *Mefp-1* in solution with the use of dynamic light scattering (DLS). We found that addition of Cu^{2+}, but not Mn^{2+}, induced the formation of larger DLS-detectable aggregates. Minor aggregate formation was found with $NaIO_4$ [42]. In these studies, we were, however, not able to distinguish between Cu^{2+}-induced oxidation of DOPA and complex formation between Cu^{2+} and DOPA. The aim of the present work was to investigate the chemical origin of Cu^{2+}-mediated cross-linking *via*

the chemical information contained in infrared absorption of differently treated adsorbed *Mefp-1* films using Attenuated Total Reflection Fourier Transform Infrared Spectroscopy (ATR-FTIR). The changes in IR absorption induced by Cu^{2+}-mediated cross-linking of adsorbed *Mefp-1* is compared with changes induced by $NaIO_4$, which is known to transform DOPA into the *o*-quinone.

MATERIALS AND METHODS

Preparation of surfaces. The ZnSe crystal was cleaned between each measurement in a 0.5% SDS solution for 30 min. This was followed by careful rinsing in milli-Q water (Millipore, Molsheim, France) and cleaning in an UV/ozone chamber for 5 min followed by rinsing in Milli-Q water and additional cleaning in the UV/ozone chamber for 5 min.

Preparation of solutions. The mussel adhesive protein Mefp-1 was purchased from Biopolymer Products AB, (Allingsås, Sweden). The purity of the protein was assessed by gel electrophoresis on polyacrylamide gels (5% acrylamide 0.1% N,N′-methylenebisacrylamide) containing 5% acetic acid and 8 M urea. Positive identification of Mefp-1 was achieved using both Coomassie blue and 4-nitro blue tetrazolium chloride (NBT) stains (for identification of DOPA-containing proteins). No impurities from other proteins were detected using this method.

Prior to measurement, *Mefp-1* was prepared in 0.1 M acetate buffer (0.075 M NaCl, pH 5.5), at a concentration of 25 μg/mL. The pH of this buffer is below the upper limit at which *Mefp-1* undergoes spontaneous oxidation and subsequent cross-linking in solution. Sodium periodate, $NaIO_4$, and Cu^{2+} were prepared in stock solutions at a concentration of 10 mM in the same buffer used for *Mefp-1*. Prior to measurements, $NaIO_4$ and Cu^{2+} was diluted to 1 mM. In all measurements, *Mefp-1* was adsorbed for 60 min followed by rinsing and subsequent cross-linking using $NaIO_4$ or Cu^{2+} for 40 min. During the first 20 min of adsorption, spectra were acquired every 5 min and after that every 20 min. Changes during cross-linking were detected by subtracting the *Mefp-1* spectrum from the cross-linked *Mefp-1* spectrum. Cu^{2+}-induced cross-linking was followed by rinsing and addition of $NaIO_4$.

ATR-FTIR measurements. A Bio-Rad FTS3000MX Fourier transform infrared spectrometer equipped with a liquid nitrogen-cooled linearized MCT detector was used to collect the FTIR spectra (Bio-Rad, Veenendaal, Netherlands). The measurements were done in ATR mode using a Pike HATR accessory. The internal reflection element was a 45° ZnSe crystal allowing five reflections at the interface with

the sample; 25 interferograms were averaged per spectrum, except for baseline subtraction where 100 interferograms were averaged with a resolution of $1\,cm^{-1}$. The useful spectral range was between 4000 and $500\,cm^{-1}$. Fluctuations in the intensity of the strong water band at $1640\,cm^{-1}$ resulted in appearance of this band in some of the difference spectra.

RESULTS AND DISCUSSION

Adsorption of Mefp-1 and assignment of absorption bands. Figure 1 shows the IR spectra in the wavenumber range between 900 and $1600\,cm^{-1}$ for *Mefp-1* after saturated adsorption (~60 minutes exposure) on a ZnSe surface*. Rinsing did not change the FTIR-spectrum, demonstrating that *Mefp-1* is irreversibly adsorbed to the ZnSe surface. The amide II band (arrow a, labeled *Amide II* in Fig. 1), associated with the C–N stretching and the N–H bending vibrations of the peptide groups, is centered at $1570\,cm^{-1}$ (between 1600 and $1490\,cm^{-1}$). In previous IR-investigations, performed on Germanium or hexadecanethiolated gold at neutral or basic pH, the amide II band of *Mefp-1* has been reported to vary between 1530 and $1550\,cm^{-1}$ [43–45]. In this investigation, *Mefp-1* was adsorbed on a ZnSe surface at pH 5.5. *Mefp-1* is a lysine-rich, positively charged protein with an extended and flexible structure in solution [35,36]. A change in pH from neutral to 5.5 will increase the positive charge of *Mefp-1*, which has a basic PI. This change probably results in conformational changes of *Mefp-1*.

The difference in position of the amide II band, therefore, most likely results from differences in experimental conditions. This interpretation is further supported by the results of Baty *et al.*, who investigated the adsorption of mussel adhesive protein (MAP) on two chemically different polymer surfaces using ATR-FTIR. The absorption pattern of MAP differed significantly on polystyrene compared with poly (octadecyl methacrylate) which was interpreted to result from different protein-surface interactions [46]. Changing the surface from germanium or hexadecanethiolated gold to ZnSe will probably contribute to the differences in spectral shape.

The strong band centered at $1472\,cm^{-1}$ (arrow b, labeled *Ring band, DOPA* in Fig. 1) is an unusual spectral feature for adsorbed proteins. A band at $1492\,cm^{-1}$ has previously been identified for *Mefp-1* adsorbed

*Fluctuations in the intensity of the strong water band at $1640\,cm^{-1}$ resulted in disappearance of the amide I band in the spectrum of adsorbed *Mefp-1*. That part of the spectrum is therefore excluded.

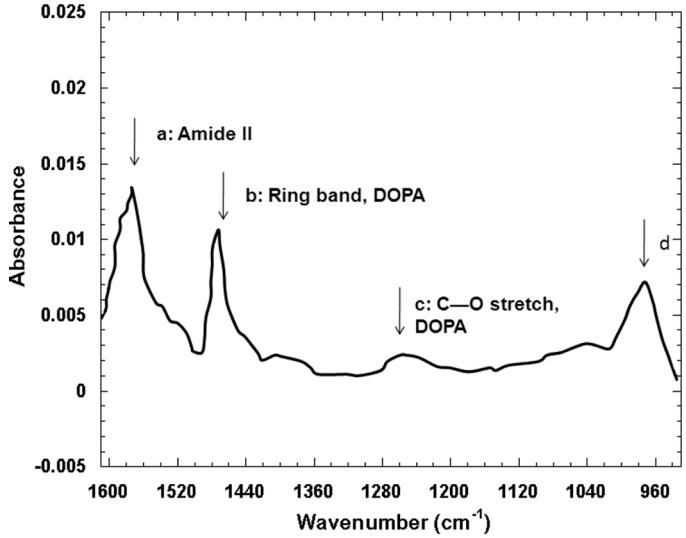

FIGURE 1 ATR-FTIR spectrum of *Mefp-1* adsorbed on the ZnSe surface. Arrows a–d indicate spectral features discussed in the text.

on a germanium surface at pH 7.2 [5,43]. Absorption in this range is expected for vibrational modes associated with substituted aromatics, of which *Mefp-1* has an unusually high content (~20%). In *Mefp-1*, approximately ~75% of the substituted aromatics are DOPA residues, which, thus, dominate the contribution to this band. The band at 1260 cm^{-1} (arrow c, labeled C–O *stretch, DOPA* in Fig. 1) has previously been associated with C–O stretching vibrations of the side chain hydroxyl groups in DOPA, catechol, and tyrosine [44,47,48]. The unusually large width of this band is due to the sensitivity of this vibration to hydrogen bonding between the side chain hydroxyl group and water [49]. Spectral features in the range 1300–1200 cm^{-1} have also been attributed to amide III vibrations which are sensitive to protein secondary structure [50]. However, our results, (see further below) in combination with the fact that *Mefp-1* essentially lacks secondary structure, strongly suggest that the band at 1260 cm^{-1} is due to C–O stretching vibrations in DOPA. The band centered at 973 cm^{-1} (arrow d in Fig. 1) is unusual for adsorbed proteins. Absorption in this region is expected for molecules including substituted phenolics and carboxylic acids. *Mefp-1* contains essentially no acidic amino acids (Glu or Asp) [51], which means that the absorption band most probably originates from the DOPA residue. However, the

absorption could originate from negatively charged acetate ions which are co-adsorbed with the positively charged *Mefp-1*.

Cross-linking of adsorbed Mefp-1. The adsorption of *Mefp-1* was followed by cross-linking using Cu^{2+} and $NaIO_4$. Changes to the IR spectrum of adsorbed *Mefp-1* 10, 20, and 40 minutes after addition of $NaIO_4$ and Cu^{2+} are shown in Figs. 2 and 3, respectively. In addition, the difference spectra acquired before the addition of reagent ($NaIO_4$ or Cu^{2+}) are shown in Figs. 2 and 3.

Concentrating initially on $NaIO_4$-mediated cross-linking (Fig. 2), an interesting spectral feature is that the bands at 1570 (arrow a), 1478 (arrow b), and 980 cm^{-1} (arrow d), increase by a factor of almost two during the cross-linking reaction. One explanation that is in qualitative agreement with this observation is that the increase in overall absorption originates from the increase in refractive index that occurs when the protein becomes more rigid and densely packed as well as the decrease in effective thickness, which was previously observed using ellipsometry [38]. It should be pointed out, though, that the increase in refractive index from 1.35 to 1.4 and decrease in thickness from ~20 to ~5 nm observed using ellipsometry, are not

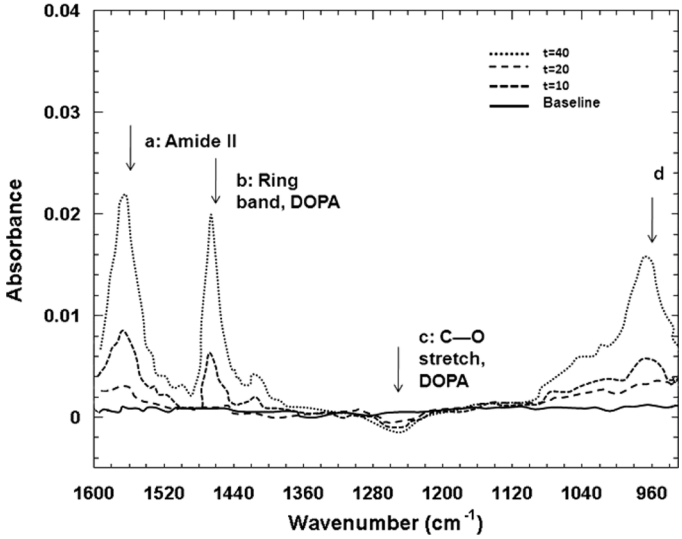

FIGURE 2 ATR-FTIR spectrum of changes in the *Mefp-1* layer induced by $NaIO_4$. Shown in the figure is the baseline (solid line), spectra taken after 10 minutes (open diamonds), 20 minutes (open triangles), and 40 minutes (open circles) of cross-linking. Arrows a–d indicate spectral changes discussed in the text.

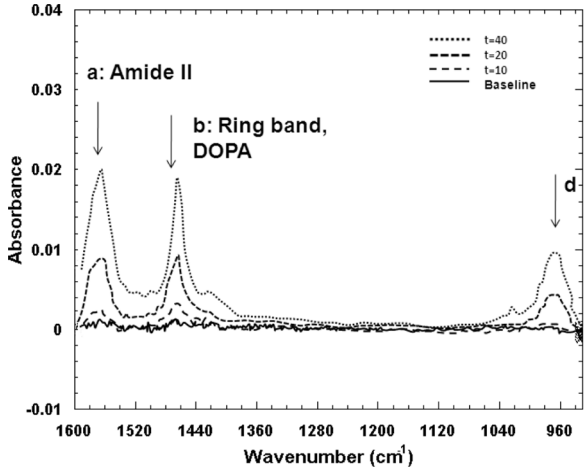

FIGURE 3 ATR-FTIR spectrum of changes in the *Mefp-1* layer induced by Cu^{2+}. Shown in the figure is the baseline (solid line), spectra taken after 10 minutes (open diamonds), 20 minutes (open triangles), and 40 minutes (open circles) of cross-linking. Arrows a–d indicate spectral changes discussed in the text.

sufficient to explain the two-fold increase in absorbance observed using ATR-FTIR. However, a strong wavelength dependence (the ellipsometry data were recorded using visible light) of the refractive index for the cross-linked film may contribute to a larger increase in absorbance upon dehydration and contraction of the protein film. At present, the available data are not sufficient to elucidate fully whether this interpretation is accurate. Since the focus of this work is entirely on the influence from cross-linking using $NaIO_4$ and Cu^{2+}, *i.e.*, on the band ($1260\,cm^{-1}$) attributed to the C–O stretching vibration of the side chain hydroxyl groups in DOPA, it was beyond the scope of this work to fully solve this somewhat peculiar observation—beyond stating that it is in qualitative agreement with previous observations.

We, thus, turn from here to the variation of the band at $1260\,cm^{-1}$ (arrow c) which, instead of increasing, fully disappears during the first 10 min of the cross-linking reaction, as evident from a negative peak in Fig. 2 with approximately the same magnitude and width as the corresponding positive peak in Fig. 1. We previously attributed this band to C–O stretching vibrations of the side chain hydroxyl groups in DOPA (see above). Since $NaIO_4$ is known to transform DOPA into the o-quinone, *i.e.*, transforming the hydroxyl groups in DOPA into carbonyl groups, it is not surprising that the band at $1260\,cm^{-1}$ disappears during the cross-linking. The disappearance of the band at

$1260\,cm^{-1}$ is a significantly more rapid process than the increase in absorption of the other bands which is attributed to the decrease in thickness and the increase in refractive index as the cross-linking reaction reaches completion. The decrease in thickness and the increase in refractive index is, thus, most likely a second step of the cross-linking reaction during which di-DOPA cross-links are formed. These results, therefore, suggest that while complete oxidation of DOPA into *o*-quinone is a rapid process, the subsequent cross-linking is a much slower process. It was not possible in previous investigations, using ellipsometry or SPR combined with the QCM-D technique, to distinguish between these two processes [38].

Turning from here to the results obtained upon Cu^{2+}-mediated cross-linking (Fig. 3) it is clear that, similar to $NaIO_4$-mediated cross-linking, the bands at 1570 (arrow a), 1478 (arrow b), and $980\,cm^{-1}$ (arrow d) increase while there is no detectable change in the DOPA band at $1260\,cm^{-1}$. The overall signature for cross-linking, interpreted as a decrease in film thickness and increase in refractive index, is clearly the same for both Cu^{2+} and $NaIO_4$-induced cross-linking, except that the magnitude of the overall absorbance increase is slightly lower for Cu^{2+}. The latter observation is supported by previous QCM-D data, which demonstrated that Cu^{2+} has a slightly less pronounced effect on the contraction of adsorbed *Mefp-1* films compared with $NaIO_4$ [42]. More interesting is, however, the complete absence of changes in the absorption band at $1260\,cm^{-1}$. Cu^{2+} has two possible mechanisms for the cross-linking. One is to initiate the same reaction as $NaIO_4$ or the byssal enzyme catechol oxidase, *i.e.*, transformation of the catechol functionality of DOPA into a *o*-quinone [41]. This would change the C–O bonds of the side chain hydroxyl groups into C=O bonds and the band at $1260\,cm^{-1}$ should disappear in accordance with $NaIO_4$-induced cross-linking. The other possible mechanism for Cu^{2+}-induced cross-linking is complex formation between Cu^{2+} and DOPA. In this case, the C–O bonds of the side chain hydroxyl groups in DOPA should be unaffected, and the band at $1260\,cm^{-1}$ would, thus, remain unchanged. This has previously been shown for complex formation between catechol and Al^{3+}, by McBride and Wesselink, who demonstrated that both free catechol and catechol complexed with Al^{3+} absorbs at $1260\,cm^{-1}$ [48]. Thus, our results suggest that the dominating mechanism of Cu^{2+} is complex formation with DOPA, rather than transformation of DOPA into the *o*-quinone. However, the overall increase in absorption observed for all other bands should have a similar influence on the magnitude of the absorption band at $1260\,cm^{-1}$. Therefore, if the C–O stretch of DOPA is completely unaffected, an increase in absorption would be

expected. Since this is not observed, it cannot be excluded that a fraction of the DOPA residues have been transformed into *o*-quinones by Cu^{2+}. Under all circumstances, a significant part of the contraction of the protein film, here observed as an increase in the overall absorption and in previous studies as a decrease in effective thickness and an increase in refractive index and shear viscosity, must be mediated by complex formation between Cu^{2+} and DOPA. The increase in density during the cross-linking demonstrates that Cu^{2+} forms complexes with two or more DOPA. Cu^{2+} is, therefore, very likely to form cross-links within and between the proteins similar to di-DOPA cross-links and, thus, contribute to the cohesive properties of the byssus.

Addition of $NaIO_4$ after Cu^{2+}-induced cross-linking. In order to investigate the stability of the Cu^{2+}-DOPA complexes towards oxidation, $NaIO_4$ was added after saturated reaction between *Mefp-1* and Cu^{2+}. Figure 4 shows the FTIR spectrum taken 30 minutes after addition of $NaIO_4$ to adsorbed *Mefp-1* pre-incubated in Cu^{2+} (*cf*. Fig. 2). The band attributed to the C−O stretching vibration in DOPA at 1260 cm^{-1} (arrow c) decreases upon addition of $NaIO_4$ to the Cu^{2+} cross-linked *Mefp-1* layer, while the other bands increase slightly. The latter

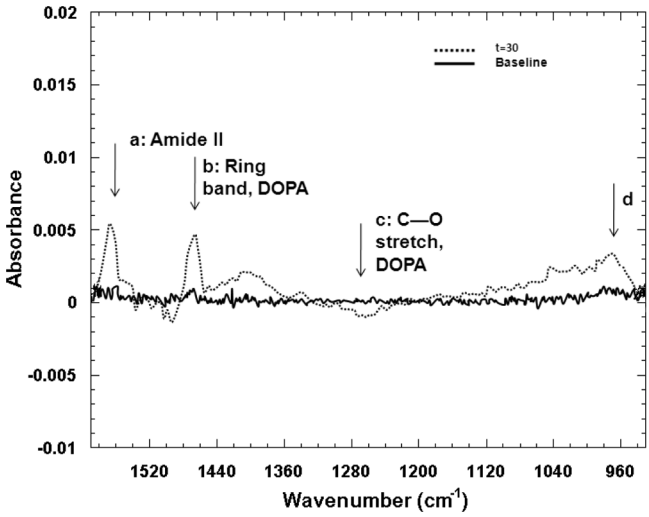

FIGURE 4 ATR-FTIR spectrum of changes in the Cu^{2+} cross-linked *Mefp-1* layer induced by $NaIO_4$. Shown in the figure is the baseline (solid line) and the spectrum taken after 30 minutes (open circles). Arrows a–d indicate spectral changes discussed in the text.

signals additional contraction and increase in optical density upon addition of $NaIO_4$, while there are two likely explanations for the former phenomenon. Firstly, formation of complexes between DOPA and Cu^{2+} may be reversible, allowing $NaIO_4$ to replace Cu^{2+} during the oxidation process. Alternatively, oxidation of DOPA is possible for the DOPA complex bound with Cu^{2+}. It is difficult from the present data to rule out one of the two possible mechanisms, but it is evident that a significant fraction of DOPA residues undergo oxidation even in the presence of Cu^{2+}, as shown in Fig. 5. The role of metal accumulation in the mussel byssus is debatable. The accumulation of metals results from active secretion during the formation of the byssal threads and not by passive absorption of metal ions from sea water [52]. It has, therefore, been suggested that accumulation of metal ions works as a detoxification process in the animal. However, the picture of the *in-vivo* adhesive formation and corresponding cross-linking is not as easy to determine if it is *via* metal complexation or oxidative di-DOPA formation. Recently Lauren and Wilker demonstrated synergistic effects between metals and $NaIO_4$ [53]. Thus, a mixture of pathway A and B as shown in Fig. 5 might result in the best adhesive and cohesive properties of the byssus. Another result demonstrating the complexity of the process was published by Lin and coworkers [54]. The adhesive properties of Mytilus edulis foot proteins *Mefp-1* and *Mefp-3* (denoted mfp-1 and mfp-3 in their study) were directly measured at the nano-scale by using a surface forces apparatus (SFA). While considerable adhesion was measured with mfp-3 no adhesion was measured

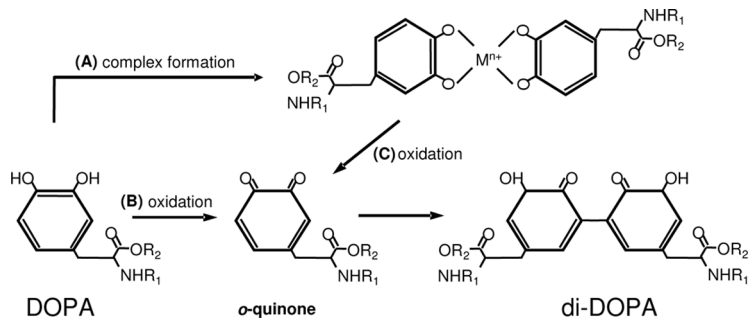

FIGURE 5 Possible reaction pathways for cross-linking of DOPA. (**A**) complex formation between transition metal ions and DOPA. (**B**) Formation of di-DOPA cross-links. DOPA is oxidized into the reactive *o*-quionone. In nature, the reaction is catalyzed by catechol oxidase, but it can also be induced by mushroom tyorsinase or sodium periodate (NaIO4). (**C**) Oxidation after complex formation.

using mfp-1, although the two proteins contain equal amounts of DOPA. The results in their study demonstrate the importance of not only understanding the cross-linking chemistry but also understanding the cross-linking "conformation" of the protein.

It should be stressed that the pH of sea water is around 8, whereas the experiments in this investigation were made at pH 5.5. The *Mefp-1* preparation, isolated from the foot, rapidly becomes spontaneously oxidized and unstable at pH over 7 [54]. On the other hand, the pH in the Mefp1-producing foot glands is low, possibly to ensure absence of auto-oxidation of Mefp 1 [54]. Thus, the higher "marine" pH is not reached until the byssus thread is completely assembled and released from the foot. Thus, the conclusion made from this *in-vitro* investigation is not affected by performing the experiments at pH 5.5, rather than at the "marine" pH.

CONCLUSIONS

In conclusion, it is judged from the present results that oxidation of DOPA into *o*-quinones is a rapid process, preceding the formation of di-DOPA cross-links and the associated protein film contraction. Similarly, complex formation between DOPA and Cu^{2+} also forms cross-links and contracts the protein film, but slightly less efficiently. Our results show that oxidation of DOPA is still possible after the formation of complexes between DOPA and Cu^{2+}. This suggests that the enzymatic oxidation of DOPA followed by formation of di-DOPA cross-links, which in nature is accomplished by the enzyme catechol oxidase, is the most important process in order to achieve good cohesive properties in the byssus.

ACKNOWLEDGMENT

This work was largely inspired by the pioneering work of Professor Waite. Indriati Pfeiffer is acknowledged for instructions regarding the use of the FTIR equipment. The Biomaterial Consortium, the New Marine Paint program (NMP), and the Biomimetic Material Science program, funded by the Foundation of Strategic Research (SSF) and MISTRA, have financially supported this work.

REFERENCES

[1] Rzepecki, L. M., Hansen, K. M., and Waite, J. H., *Biol. Bull.* **183**, 123–137 (1992).
[2] Waite, J. H., *Biol. Rev.* **58**, 209–231 (1983).

[3] Haemers, S., van der Leeden, M. C., Koper, G. J. M., and Frens, G., *Langmuir* **18**, 4903–4907 (2002).
[4] Frank, B. P. and Belfort, G., *Biotechnol. Prog.* **18**, 580–586 (2002).
[5] Suci, P. A. and Geesey, G. G., *Colloid Surf. B-Biointerfaces* **22**, 159–168 (2001).
[6] Haemers, S., van der Leeden, M. C., Nijman, E. J., and Frens, G., *Colloid Surf. A-Physicochem. Eng. Asp.* **190**, 193–203 (2001).
[7] Burzio, L. A. and Waite, J. H., *Biochemistry* **39**, 11147–11153 (2000).
[8] Even, M. A., Wang, J., and Chen, Z., *Langmuir* **24**, 5795–5801 (2008).
[9] Berglin, M. and Gatenholm, P., *J. Adhes. Sci. Technol.* **13**, 713–727 (1999).
[10] Berglin, M. and Gatenholm, P., *Colloid Surf. B-Biointerfaces* **28**, 107–117 (2003).
[11] Strausberg, R. L. and Link, R. P., *Trends Biotechnol.* **8**, 53–57 (1990).
[12] Holten-Andersen, N. and Waite, J. H., *J. Dent. Res.* **87**, 701–709 (2008).
[13] Norton, L. A., Andersen, K. L., Arenholtbindslev, D., Andersen, L., and Melsen, B., *Arch. Oral Biol.* **40**, 863–872 (1995).
[14] Renardrooney, D. C., Hajnoczky, G., Seitz, M. B., Schneider, T. G., and Thomas, A. P., *J. Biol. Chem.* **268**, 23601–23610 (1993).
[15] Vreeland, V., Waite, J., and Epstein, L., *J. Phycol.* **34**, 1–8 (1998).
[16] Waite, J. H. and Qin, X. X., *Biochemistry* **40**, 2887–2893 (2001).
[17] Waite, J. H., *Integr. Comp. Biol.* **42**, 1172–1180 (2002).
[18] Waite, J. H. and Tanzer, M. L., *Science* **212**, 1038–1040 (1981).
[19] Taylor, S. W., Waite, J. H., Ross, M. M., Shabanowitz, J., and Hunt, D. F., *J. Am. Chem. Soc.* **116**, 10803–10804 (1994).
[20] Papov, V. V., Diamond, T. V., Biemann, K., and Waite, J. H., *J. Biol. Chem.* **270**, 20183–20192 (1995).
[21] Lee, H., Scherer, N. F., and Messersmith, P. B., *Proc. Natl. Acad. Sci. U.S.A.* **103**, 12999–13003 (2006).
[22] McDowell, L. M., Burzio, L. A., Waite, J. H., and Schaefer, J., *J. Biol. Chem.* **274**, 20293–20295 (1999).
[23] Waite, J. H., *Int. J. Biol. Macromol.* **12**, 139–144 (1990).
[24] Suzuki, S., Yamaguchi, K., Nakamura, N., Tagawa, Y., Kuma, H., and Kawamoto, T., *Inorg. Chim. Acta* **283**, 260–267 (1998).
[25] Albrecht, M., *Chem. Soc. Rev.* **27**, 281–287 (1998).
[26] Szefer, P., Kim, B. S., Kim, C. K., Kim, E. H., and Lee, C. B., *Environ. Polut.* **129**, 209–228 (2004).
[27] Szefer, P., Frelek, K., Szefer, K., Lee, C. B., Kim, B. S., Warzocha, J., Zdrojewska, I., and Ciesielski, T., *Environ. Polut.* **120**, 423–444 (2002).
[28] Swann, C. P., Adewole, T., and Waite, J. H., *Comp. Biochem. Phys. B* **119**, 755–759 (1998).
[29] Gundacker, C., *Chemosphere* **38**, 3339–3356 (1999).
[30] Holten-Andersen, N., Mates, T. E., Toprak, M. S., Stucky, G. D., Zok, F. W., and Waite, H. J., *Langmuir* **25**, 3323–3326 (2009).
[31] Taylor, S. W., Chase, D. B., Emptage, M. H., Nelson, M. J., and Waite, J. H., *Inorg. Chem.* **35**, 7572–7577 (1996).
[32] Taylor, S. W., Luther, G. W., and Waite, J. H., *Inorg. Chem.* **33**, 5819–5824 (1994).
[33] Waite, J. H., *J. Biol. Chem.* **258**, 2911–2915 (1983).
[34] Waite, J. H., Housley, T. J., and Tanzer, M. L., *Biochemistry* **24**, 5010–5014 (1985).
[35] Deacon, M. P., Davis, S. S., Waite, J. H., and Harding, S. E., *Biochemistry* **37**, 14108–14112 (1998).
[36] Haemers, S., van der Leeden, M. C., and Frens, G., *Biomaterials* **26**, 1231–1236 (2005).

[37] Fant, C., Sott, K., Elwing, H., and Hook, F., *Biofouling* **16**, 119–132 (2000).
[38] Hook, F., Kasemo, B., Nylander, T., Fant, C., Sott, K., and Elwing, H., *Anal. Chem.* **73**, 5796–5804 (2001).
[39] Waite, J. H., *J. Mar. Biol. Assoc. U.K.* **65**, 359–372 (1985).
[40] Cabanes, J., Garciacanovas, F., and Garciacarmona, F., *Acta Biochim. Biophys.* **914**, 190–197 (1987).
[41] Balla, J., Kiss, T., and Jameson, R. F., *Inorg. Chem.* **31**, 58–62 (1992).
[42] Hedlund, J., Andersson, M., Fant, C., Bitton, R., Bianco-Peled, H., Elwing, H., and Berglin, M., *Biomacromolecules* **10**, 845–849 (2009).
[43] Suci, P. A. and Geesey, G. G., *J. Colloid Interface Sci.* **230**, 340–348 (2000).
[44] Olivieri, M. P., Loomis, R. E., Meyer, A. E., and Baier, R. E., *J. Adhes. Sci. Technol.* **4**, 197–204 (1990).
[45] Harder, P., Grunze, M., and Waite, J. H., *J. Adhes.* **73**, 161–177 (2000).
[46] Baty, A. M., Suci, P. A., Tyler, B. J., and Geesey, G. G., *J. Colloid Interface Sci.* **177**, 307–315 (1996).
[47] Olivieri, M. P., Rittle, K. H., Tweden, K. S., and Loomis, R. E., *Biomaterials* **13**, 201–208 (1992).
[48] McBride, M. B. and Wesselink, L. G., *Environ. Sci. Technol.* **22**, 703–708 (1988).
[49] Barth, A., *Prog. in Biophys. & Mol. Bio.* **74**, 141–173 (2000).
[50] Chittur, K. K., *Biomaterials* **19**, 357–369 (1998).
[51] Filpula, D. R., Lee, S. M., Link, R. P., Strausberg, S. L., and Strausberg, R. L., *Biotechnol. Prog.* **6**, 171–177 (1990).
[52] George, S. G., Pirie, B. J. S., and Coombs, T. L., *J. Exp. Mar. Biol. Ecol.* **23**, 71–84 (1976).
[53] Lauren, M. H. and Wilker, J. J., *J. Matr. Sci.* **42**, 8934–8942 (2007).
[54] Lin, Q., Gourdon, D., Sun, C. J., Holten-Andersen, N., Anderson, T. H., Waite, J. H., and Israelachvili, J. N., *Proc. Natl. Acad. Sci. U.S.A.* **104**, 3782–3786 (2007).